ACS APPLIED MATERIALS & INTERFACES

www.acsami.org

Research Article

Alkanethiol Monolayer End Groups Affect the Long-Term Operational Stability and Signaling of Electrochemical, Aptamer-Based Sensors in Biological Fluids

Alexander Shaver, Samuel D. Curtis, and Netzahualcóyotl Arroyo-Currás*

Cite This: *ACS Appl. Mater. Interfaces* 2020, 12, 11214–11223

Read Online

ACCESS | Metrics & More | Article Recommendations | Supporting Information

ABSTRACT: Electrochemical aptamer-based (E-AB) sensors achieve highly precise measurements of specific molecular targets in untreated biological fluids. This unique ability, together with their measurement frequency of seconds or faster, has enabled the real-time monitoring of drug pharmacokinetics in live animals with unprecedented temporal resolution. However, one important weakness of E-AB sensors is that their bioelectronic interface degrades upon continuous electrochemical interrogation—a process typically seen as a drop in faradaic and an increase in charging currents over time. This progressive degradation limits their in vivo operational life to 12 h at best, a period that is much shorter than the elimination half-life of the vast majority of drugs in humans. Thus, there is a critical need to develop novel E-AB interfaces that resist continuous electrochemical interrogation in biological fluids for prolonged periods. In response, our group is pursuing the development of better packed, more stable self-assembled monolayers (SAMs) to improve the signaling and extend the operational life of in vivo E-AB sensors from hours to days. By invoking hydrophobicity arguments, we have created SAMs that do not desorb from the electrode surface in aqueous physiological solutions and biological fluids. These SAMs, formed from 1-hexanethiol solutions, decrease the voltammetric charging currents of E-AB sensors by 3-fold relative to standard monolayers of 6-mercapto-1-hexanol, increase the total faradaic current, and alter the electron transfer kinetics of the platform. Moreover, the stability of our new SAMs enables uninterrupted, continuous E-AB interrogation for several days in biological fluids, like undiluted serum, at a physiological temperature of 37 °C.

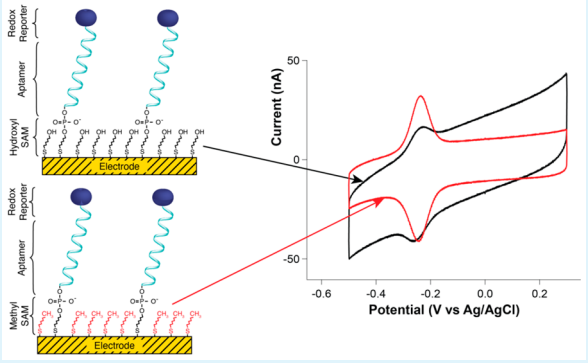

KEYWORDS: *voltammetry, self-assembled monolayer, biosensor, DNA, hexanethiol*

INTRODUCTION

Alkanethiol self-assembled monolayers (SAMs) are employed in gold-supported bioelectronic interfaces to decrease the nonspecific adsorption of proteins and other biomolecules.[1−4] SAMs are also exploited as molecular blocking layers to improve the signal-to-noise ratio of electrochemical measurements that depend on surface-bound redox reporters.[5] This effect occurs because SAMs act as length-tunable insulators[6] that extend the dielectric distance between an electrode and the electrolyte, decreasing double layer capacitance.[7] Therefore, SAMs dramatically decrease the charging currents measured by, for example, voltammetry,[8] which can mask faradaic currents originating from surface-bound redox reporters. Also, because SAMs occupy the majority of electroactive sites available on a gold surface,[9] they prevent the occurrence of undesired, gold-electrocatalyzed reactions at low voltages, such as the reduction of molecular oxygen.[10] Thus, alkanethiol SAMs enable the high signal-to-noise electrochemical interrogation of bioelectronic interfaces for prolonged times in biological fluids.

Electrochemical, aptamer-based (E-AB) sensors are a sensing technology that exploits alkanethiol SAMs for their surface-blocking and antifouling properties.[11] E-AB sensors consist of three main components: (1) an electrode-blocking SAM, (2) electrode-bound, target-binding nucleic acid aptamers, and (3) redox reporters (Figure 1A). The reporters are covalently attached to the aptamers using various linker chemistries, most commonly via a phosphodiester bond.[12] The aptamers are similarly attached to the SAM. In the presence of target, E-AB sensors undergo a binding-induced conformational change that, in turn, causes a change in electron transfer between the reporter and the electrode that can be measured electrochemically.[13] For example, the binding of tobramycin to aminoglycoside detecting E-AB sensors is observed as an

Received: December 10, 2019
Accepted: February 10, 2020
Published: February 10, 2020

https://dx.doi.org/10.1021/acsami.9b22385
ACS Appl. Mater. Interfaces 2020, 12, 11214–11223

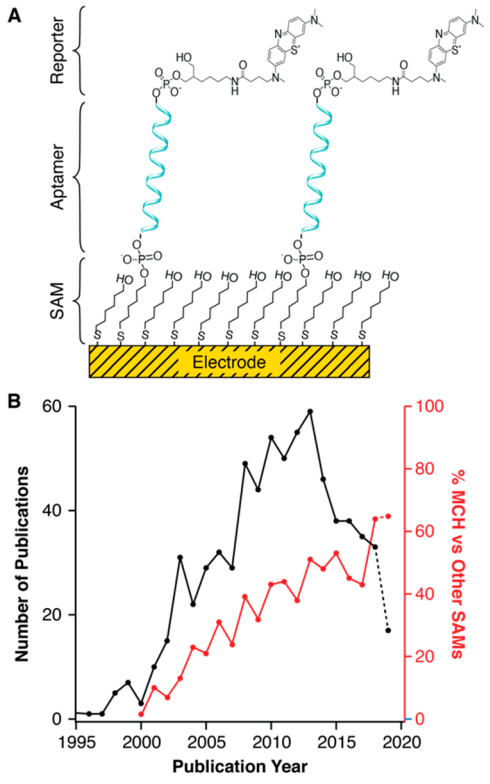

Figure 1. The anatomy of E-AB sensors. (A) They can be dissected into three main components: an electrode blocking alkanethiol SAM, a target-binding nucleic acid aptamer, and a redox reporter. The aptamer is covalently bound at the 5′ end to an alkanethiol linker and at the 3′ end to the reporter (here a modified methylene blue tethered to a phosphodiester via an amide bond). (B) The SAM's end groups can dramatically affect the operational life, signaling, and signal-to-noise ratio of not only E-AB sensors but also of nucleic acid–based electrochemical sensors in general. This fact notwithstanding, a significant fraction of the published literature has focused on the use of just one hydroxyl-terminated SAM, 6-mercapto-1-hexanol (MCH). The SciFinder search terms used to create panel B are provided as Supporting Information. The red trace represents the percentage of total publications (in black) that have reported the use of MCH as a blocking SAM.

increase in peak current or in the area under square-wave voltammograms.[14] Because of their architecture, the signaling of E-AB sensors is strongly affected by the organization and thickness of the SAM employed.[15] Moreover, the SAM's end groups are not inert but can affect the signaling of E-AB sensors,[16,17] and the stability of the SAM affects their shelf and working life.[18,19] Therefore, the development of tightly packed, biocompatible, multiday-stable monolayers is key to achieving high signal-to-noise E-AB measurements for prolonged times.

E-AB sensors already support continuous, real-time measurements of specific molecular targets in situ in live animals.[20] However, the duration of these measurements is limited to a few hours, in part because of biofouling,[4] but also because of progressive sensor degradation resulting from continuous electrochemical interrogation in biological fluids. To overcome this progressive degradation and enable multihour E-AB sensing in vivo, prior works have sought to differentially correct drift in real time by using dual-labeled aptamers[21,22] or multifrequency interrogation approaches.[20,23,24] Although effective at correcting E-AB drift, these engineering strategies do not stop chemical degradation of the sensor. In response, here we demonstrate that the stability of the blocking SAM plays an important role in E-AB sensor life, and that by carefully selecting the SAM's end group we not only produce longer-lasting monolayers (and, therefore, E-AB sensors) but also tune electron-transfer kinetics and improve the signal-to-noise ratio of E-AB measurements.

RESULTS AND DISCUSSION

From the first described E-AB sensor[25] until now, the great majority of E-AB sensor-related studies report the use of 6-mercapto-1-hexanol (MCH) as the electrode-blocking SAM. Moreover, MCH has been extensively used to form SAMs in other kinds of DNA-based sensors[26] as well as in unrelated analytical platforms based on, for example, gold nanoparticles.[27] This trend continues today with the use of MCH reported in ∼60% of all DNA-based electrochemical biosensor works published in 2019 (Figure 1B). Only a few studies have investigated the effect of different monolayer end groups, such as carboxyl-, sulfonate-, or amine-terminated alkanethiols, on the performance of E-AB sensors.[17,28] To the best of our knowledge, no prior work has studied how methyl-terminated alkanethiols affect E-AB signaling. This fact remains despite pioneering work by Chidsey and Loiacono,[16] indicating that methyl-terminated alkanethiols form SAMs with superior packing and fewer defects over carboxyl-, hydroxyl-, or nitrile-terminated monolayers. The work of Poirier and colleagues[29,30] further supports this conclusion through the use of high-resolution scanning tunneling microscopy to reveal a great extent of monolayer disorder when MCH is exposed to water vapor. Additionally, recent work by Fies and colleagues[31] reveals increased water penetration in hydrophilic monolayers compared to hydrophobic monolayers. Motivated by these previous reports, we hypothesized that decreasing the solubility and wettability of E-AB SAMs through the use of methyl-terminated alkanethiols would improve both monolayer packing and stability, thereby improving the operational life and performance of E-AB sensors.

We first tested our hypothesis by confirming that methyl-terminated alkanethiols reduce the charging current observed in voltammetrically interrogated E-AB sensors. As our test bed, we used 1-hexanethiol (HxSH), the methyl-terminated analogue of MCH. For these experiments, we incubated gold electrodes in aqueous solutions containing either MCH or HxSH for 15 h. We then rinsed the electrodes with deionized water, immersed them in thiol-free phosphate-buffered saline, and interrogated them using cyclic voltammetry. These measurements confirmed that both monolayers achieve total suppression of the oxygen reduction reaction and that the charging current observed in MCH- and HxSH-modified electrodes was 1 and 2 orders of magnitude, respectively, below that of bare gold electrodes (Figure 2A). They also confirmed that monolayer packing was significantly tighter for HxSH, dropping the charging current from 25 ± 5 nA for MCH (Figure 2B, red trace) to 8 ± 2 nA for HxSH (Figure 2C, red trace). The same observations held true when we functionalized the electrodes with a mixture of MCH- or HxSH-modified and DNA-modified SAMs (black traces in Figure 2B,C) via coincubation, indicating that the surface packing (i.e., the charging current) of HxSH is unaffected by the surface-attachment of DNA.

Beyond improving monolayer packing, HxSH SAMs are more stable than MCH SAMs under continuous voltammetric interrogation. To demonstrate this, we fabricated E-AB sensors

https://dx.doi.org/10.1021/acsami.9b22385
ACS Appl. Mater. Interfaces 2020, 12, 11214−11223

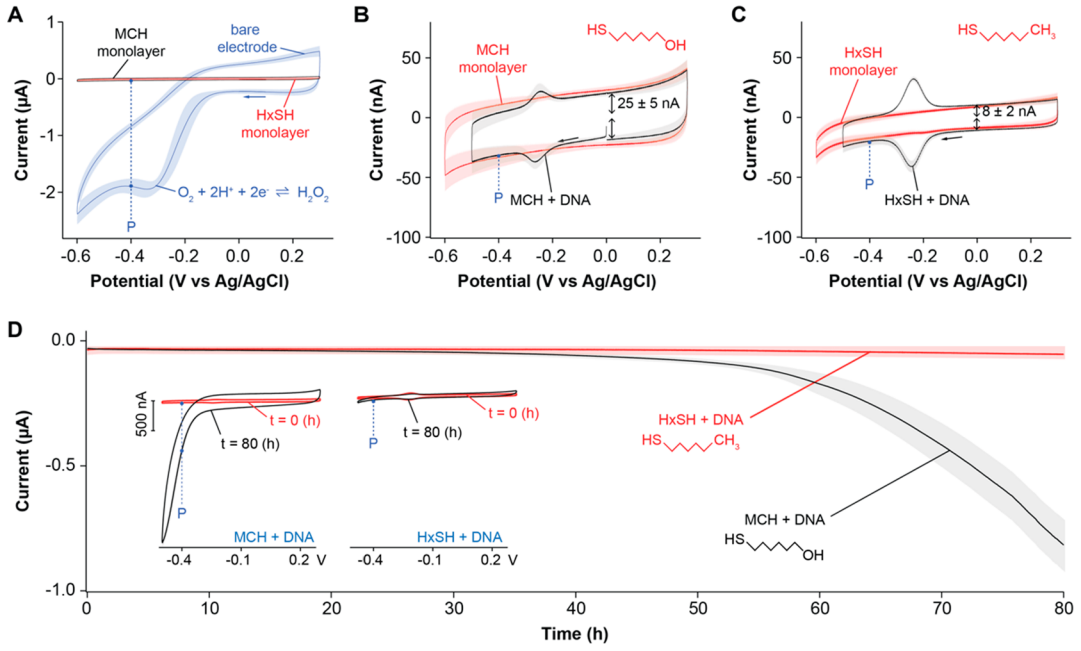

Figure 2. Methyl-terminated SAMs achieve tighter packing and longer stability relative to hydroxyl-terminated SAMs. (A) Relative to bare gold, both MCH and HxSH SAMs achieve total suppression of the oxygen reduction reaction, shown here in blue. However, the surface packing of such monolayers is not equally tight, and although MCH SAMs (B) decrease charging currents by 1 order of magnitude relative to bare electrodes, HxSH SAMs (C) achieve superior surface packing, dropping the charging currents by 2 orders of magnitude. (D) Moreover, the hydrophobicity of HxSH prevents its desorption over time even under continuous electrochemical interrogation. The insets show the first (t = 0 h) and last (t = 80 h) voltammograms recorded on MCH- (left) and HxSH-modified (right) electrodes. The label P indicates the voltage probe of −0.4 V we used to measure the faradaic contribution of the oxygen reduction reaction to the total voltammetric current as the monolayers degraded over time. The long traces correspond to the current measured at P for voltammograms recorded every 40 s for a total period of 80 h. Shaded areas in all panels represent the standard deviation calculated from four electrodes.

with either MCH or HxSH SAMs and serially interrogated them by cyclic voltammetry every 40 s for 80 h. Using SACMES, a Python script previously reported by our group,[32] we extracted the current from each voltammogram at a probe voltage, P = −0.4 V, where the electrochemical reduction of molecular oxygen to hydrogen peroxide occurs (Figure 2A). Monolayer desorption progressively opens electrocatalytic sites on the electrode surface, which increase the faradaic contribution from oxygen reduction to the total voltammetric current. Thus, by monitoring current at P, we determined the rate of monolayer desorption for the two SAMs. Using this method, we established that MCH SAMs undergo progressive desorption (Figure 2D, black trace) at a constant rate during the first 24 h of continuous interrogation (∼1.2% loss of monolayer coverage per hour, Figure S1). However, after that period, the rate of desorption increases by an order of magnitude until the MCH SAMs are completely desorbed from the electrode surface, after approximately 80 h (left inset, Figure 2D). The HxSH SAMs, in contrast, remain stable and virtually unchanged for the first 40 h (Figure 2D, red trace). When HxSH SAMs start to degrade, they do so at a rate of ∼1.4% loss of coverage per hour (Figure S1), comparable to that of the early stages of MCH desorption. Thus, our results agree with the observations made by Chidsey and Loiacono[16] that methyl-terminated SAMs are tightly packed and comparatively more stable than hydroxyl-terminated ones, strongly indicating that monolayer end groups can be tailored to improve the long-term stability of E-AB sensors.

At short incubation times (≤24 h), the surface packing of HxSH SAMs is superior to that of longer alkanethiol SAMs irrespective of end-group chemistry. This conclusion is based on a comparison of cyclic voltammograms measured on electrodes modified with MCH against 8-mercapto-1-octanol (MCO) and 11-Mercapto-1-undecanol (MCU) (Figure 3A), as well as HxSH against 1-octanethiol (OcSH) and 1-undecanethiol (UdSH) (Figure 3B) after 15 h long incubations in ethanolic solutions (we employed ethanol to achieve full dissolution of the longer, water-insoluble alkanethiols). Although these voltammograms reveal a slight decrease in charging current going from MCH to MCO, the same is not true for the methyl-terminated SAMs, of which HxSH produces the lowest charging current. Moreover, we observed that SAMs formed by MCU, UdSH, and OcSH did not achieve complete suppression of the oxygen reduction reaction (faradaic current on the left side of Figure 3A,B), an indication that such monolayers were not effective at covering the entire surface of the electrodes. These results indicate that HxSH forms tighter monolayers than longer thiols at relatively short incubation times (15 h).

Unlike C_8 and C_{11} methyl-terminated SAMs, HxSH monolayers are stable under continuous voltammetric interrogation for days. We fabricated HxSH-, OcSH-, and UdSH-modified electrodes using the above-described ethanolic solutions and serially interrogated them via cyclic voltammetry every 40 s for over 70 h (Figure 3C). Because of their tighter monolayer packing, the voltammetric currents measured on HxSH SAMs (∼15 nA) consisted primarily of charging current and increased by only 10% after 72 h. The currents measured from OcSH (∼55 nA) and UdSH (∼60 nA) SAMs, in contrast, contained a significant contribution of faradaic current from the oxygen reduction reaction and increased by over 20% after 72 h. We note that while longer incubation

https://dx.doi.org/10.1021/acsami.9b22385
ACS Appl. Mater. Interfaces 2020, 12, 11214−11223

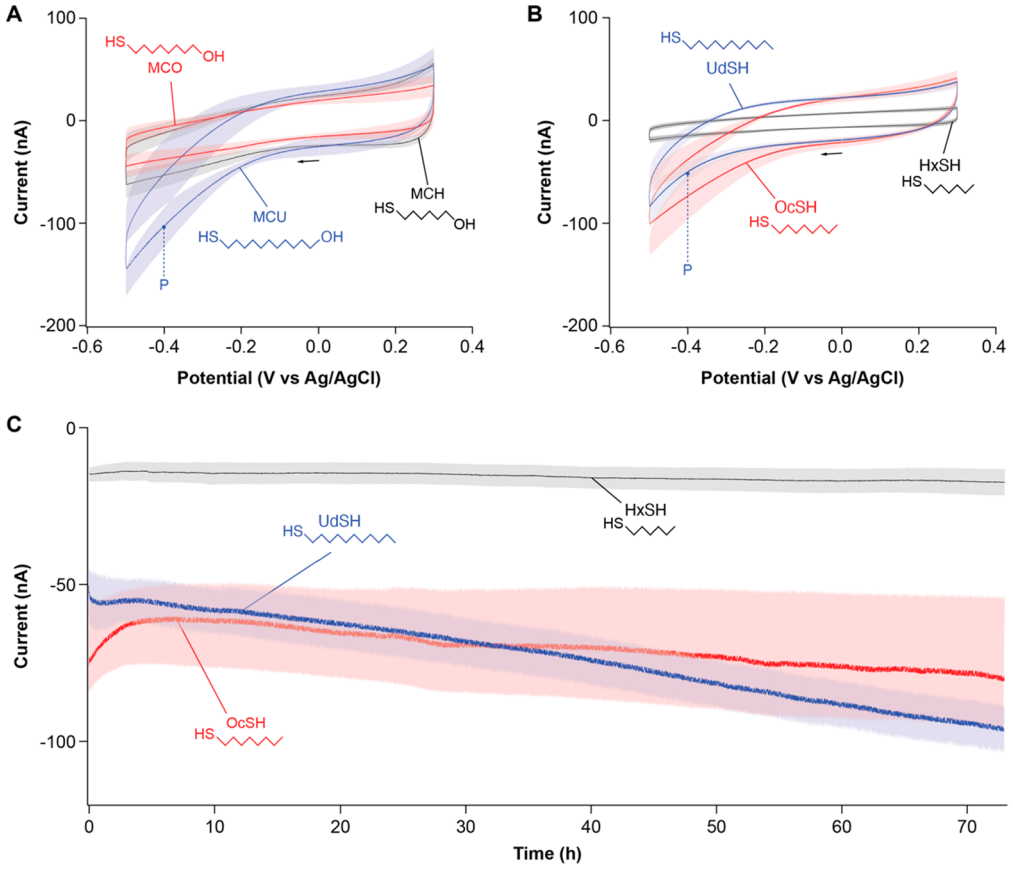

Figure 3. Six-carbon alkanethiols form tighter and more stable SAMs than longer chains at short (15 h) incubation times. Here, we compare cyclic voltammograms measured on three hydroxyl-terminated SAMs (A) 6-mercapto-1-hexanol (MCH), 8-mercapto-1-octanol (MCO), and 11-mercapto-1-undecanol (MCU); and three methyl-terminated SAMs (B) 1-hexanethiol (HxSH), 1-ocatanethiol (OcSH), and 1-undecanethiol (UdSH). (C) The stability of HxSH SAMs is not only superior to that of hydroxyl-terminated but also of longer methyl-terminated SAMs. SAMs prepared by incubations shorter than 15 h degraded faster. Shaded areas in all panels represent the standard deviation calculated from eight electrodes.

Table 1. Aptamer Sequences Employed in This Work

target	sequence	ref
aminoglycosides	5′- GGG ACT TGG TTT AGG TAA TGA GTC CC -3′	14
vancomycin	5′- CGA GGG TAC CGC AAT AGT ACT TAT TGT TCG CCT ATT GTG GGT CGG -3′	35
doxorubicin	5′- ACC ATC TGT GTA AGG GGT AAG GGG TGG T -3′	36

times could produce tighter monolayer packing for the longer, more hydrophobic SAMs,[6,33,34] measurements performed after 24 h long incubations with MCO or OcSH did not show any significant reduction of charging currents or improvement in stability compared to aqueous HxSH incubations (Figure S2). Moreover, as a pragmatic disadvantage, incubations lasting longer than 24 h become inconvenient for the rapid prototyping and fabrication of E-AB sensors. Thus, through these experiments, we determined that irrespective of monolayer end groups, SAMs formed in aqueous solutions produce tighter, more stable monolayers than those formed in ethanolic solutions, further justifying the use of HxSH in water for incubation conditions (Figure S3).

The tight monolayer packing achieved with methyl-terminated SAMs improves the signal-to-noise ratio of E-AB measurements via square wave voltammetry. This effect likely arises because, at equal surface concentration of aptamer probes (Figure S4), lower charging currents make it easier to resolve the faradaic peak derived from the reduction of surface-bound redox reporters. We prepared E-AB sensors by incubating gold electrodes in solutions containing both HxSH (or MCH) and a 26-nucleotide aptamer that binds to the aminoglycoside antibiotic tobramycin (Table 1). When we interrogated such sensors in the absence of tobramycin, we observed a significant increase in the magnitude of the voltammograms recorded on HxSH relative to MCH SAMs (Figure 4A). Specifically, interrogating HxSH surfaces at square-wave frequencies of 30 and 250 Hz produced voltammograms 67% and 250% larger relative to those recorded on MCH SAMs. In fact, we observed this current enhancement across all the square-wave frequencies we tested (Figure 4B). This enhancement, coupled to the constant charging currents achieved via increased monolayer packing and stability, allows the continuous square-wave voltammetric interrogation of HxSH-modified E-AB sensors for over 60 h (Figure 4C). In contrast, MCH-modified E-AB sensors fail after approximately 30 h, when the increasing charging currents caused by monolayer desorption become larger than

https://dx.doi.org/10.1021/acsami.9b22385
ACS Appl. Mater. Interfaces 2020, 12, 11214−11223

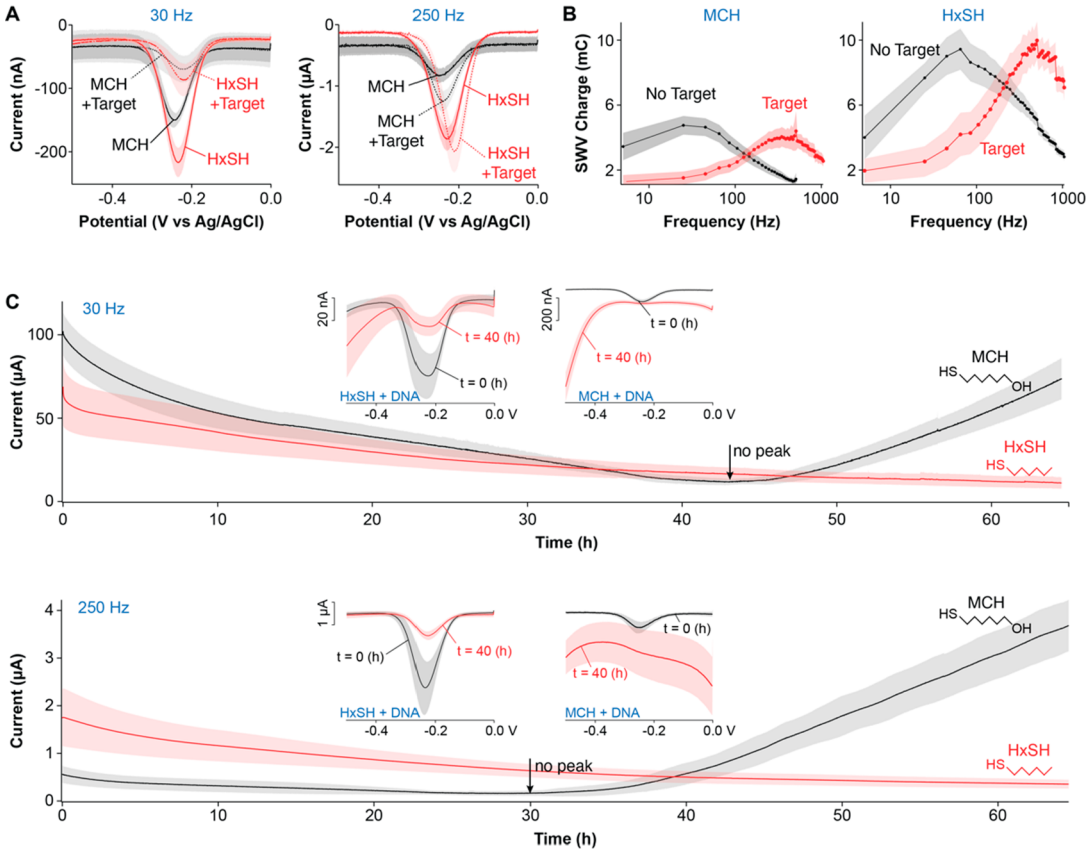

Figure 4. Methyl-terminated SAMs enhance the total signal output of E-AB sensors. We illustrate this effect using aminoglycoside-binding E-AB sensors. (A) When interrogated by square wave voltammetry, the currents measured on HxSH-modified sensors are larger in magnitude relative to MCH-modified sensors. In the absence of target (tobramycin), for example, geometry and surface area-equivalent electrodes gave 67% and 250% larger peak currents at 30 and 250 Hz, respectively, for HxSH relative to MCH SAMs. The surface coverage of aptamer probes was equivalent on both monolayers. (B) We observed such a signal increase across the entire range of square-wave frequencies we tested (see total charge magnitude in *y* axes). Moreover, the removal of the hydroxyl group accelerated electron transfer kinetics in methyl-terminated SAMs, as seen here as a shift of the position of maximum charge for HxSH to higher frequencies relative to MCH SAMs. (C) The combination of superior monolayer stability and larger baseline currents means that HxSH SAMs support continuous E-AB sensing for longer periods than MCH SAMs. At the two square-wave interrogation frequencies employed here, MCH SAMs reached a point of no peak (black arrows in both panels) tens of hours before the same point is reached with HxSH SAMs. The insets show voltammograms at t = 0 h and t = 40 h recorded on HxSH- (left) and MCH-modified (right) electrodes. Note the increase in charging current accompanied by the total disappearance of the faradaic peak. Shaded areas in all panels represent the standard deviation calculated from eight electrodes.

the faradaic peak of the redox reporter (see insets in Figure 4C).

Monolayer end groups such as hydroxyl and methyl not only affect the operational life of E-AB sensors, but also their signaling. This effect was previously reported by Ricci and colleagues for DNA-based sensors employing SAMs ending in hydroxyl, sulfonate, and amine groups.[28] Their observations indicate that positively charged end groups (tertiary amines) strongly interact with the negatively charged backbone of DNA, increasing E-AB sensor gain. However, little is known about how hydrophobic surfaces can affect E-AB signaling. In response, we comparatively studied E-AB signaling on HxSH- relative to MCH-modified sensors. We fabricated three different batches of E-AB sensors, each employing aptamers binding to doxorubicin, vancomycin, or tobramycin, using previously reported sequences (Table 1).[14,35,36] To identify optimal square-wave frequency pairs for the interrogation of these sensors, we built "quasi-reversible maximum" maps as initially described by Lovriç and colleagues (Figures 4B and S5).[37,38] From these maps, we were able to identify the existence of two electron-transferring states (i.e., two maxima, each corresponding to either unbound or target-bound aptamers) for each sensor type. We selected the frequency corresponding to these maxima to interrogate our E-AB sensors.

Removing the hydroxyl end group from the E-AB SAMs causes a change in signaling that strongly depends on aptamer sequence. For the cases of doxorubicin- (Figure 5A) and vancomycin-binding (Figure 5B) E-AB sensors, for example, the calibration curves showed an inversion of E-AB signaling behavior between MCH and HxSH monolayers. Specifically, at the high square-wave frequency, we observed a flip from increasing current with increasing target concentration, to decreasing current. The inverse was observed for the low square-wave frequency. This behavior is difficult to explain, but we speculate three possible origins: (1) The secondary structure of the unbound aptamer receptors could change from the unfolded state on MCH surfaces to a folded state on HxSH surfaces, the latter of which would unfold upon target binding; (2) In the case of HxSH, the receptors may switch between two folded states with different electron transfer kinetics; or (3) The redox reporter, methylene blue, may

https://dx.doi.org/10.1021/acsami.9b22385
ACS Appl. Mater. Interfaces 2020, 12, 11214−11223

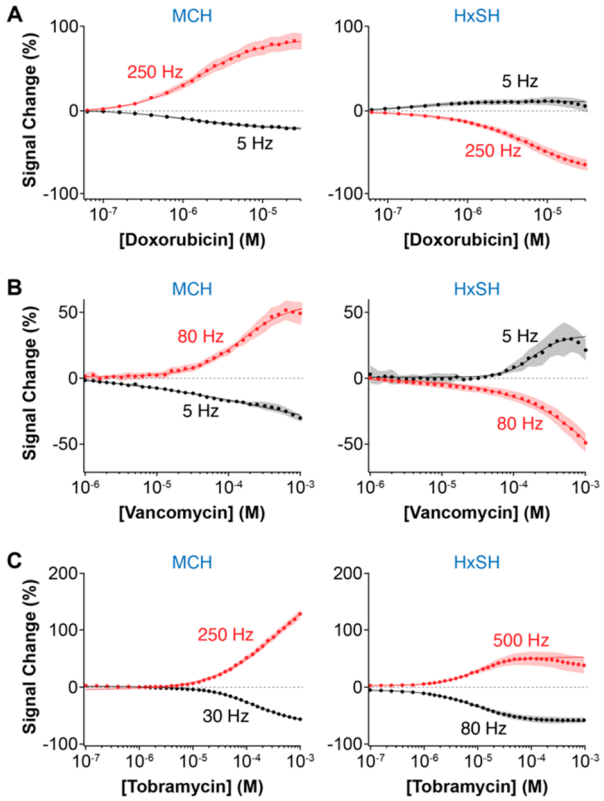

Figure 5. Methyl- and hydroxyl-terminated monolayers produce different and, in some cases, opposing E-AB signaling with increasing target concentrations. We illustrate this effect by presenting calibration curves built with E-AB sensors binding to (A) the chemotherapeutic doxorubicin, (B) the glycopeptide vancomycin, and (C) the aminoglycoside antibiotic tobramycin. Although the molecular structures and chemical properties of these targets are very different, as well as the folded conformations of their aptamers, the removal of hydroxyl groups from MCH to HxSH clearly has a profound effect on E-AB signaling. We speculate that the different behaviors observed are due to monolayer-induced changes in the folded conformations of the aptamers, which in turn change the local environment of the aptamer's binding pocket and the redox reporter (here methylene blue), and of E-AB electron transfer kinetics. While there was minimal change in the apparent dissociation constant for vancomycin (HxSH K_D = 187 ± 18 μM; MCH K_D = 151 ± 9 μM), the apparent dissociation constant for doxorubicin worsened from MCH (K_D = 1.63 ± 0.05 μM) to HxSH (K_D = 15.8 ± 0.8 μM), and the apparent dissociation constant for tobramycin improved from MCH (K_D = 154 ± 2 μM) to HxSH (K_D = 9.8 ± 0.3 μM). Shaded areas in all panels represent the standard deviation calculated from eight electrodes. Solid lines represent nonlinear fits of the data to the Hill isotherm.

interact differently with MCH and HxSH due to the fact that it contains both a positive charge and hydrophobic rings. These differential interactions would affect electron transfer rates and, thus, E-AB signaling. If either 1 or 2 is true, the secondary structure of the receptors must be affected by hydrogen bonding between the phosphate backbone of the DNA aptamers and the hydroxyl groups in MCH. Moreover, the observed effect could be due to a change in the ζ potential of the monolayer, from being negatively charged in MCH SAMs[17] to presumably neutral on HxSH SAMs.

The absence of hydroxyl end groups in HxSH did not cause an inversion of signaling in the case of aminoglycoside-detecting E-AB sensors but, instead, accelerated the reporter's electron transfer kinetics. This acceleration is seen as a shift of charge maxima to higher frequencies by 160 Hz in quasi-reversible maps (Figure 4B), relative to E-AB sensors functionalized with MCH. Moreover, HxSH-functionalized E-AB sensors presented a lower apparent dissociation constant (Figure 5C), K_D, going from 154 ± 2 μM on MCH to 9.8 ± 0.3 μM on HxSH. Again, we speculate that these changes in electron transfer kinetics and apparent binding constants are related to monolayer-induced changes in the preferred folded conformation of the aptamer or in the local environment of the reporter (for example, by bringing it closer to the electrode surface via hydrophobic interactions with HxSH). Regardless, it is clear that monolayer end groups are not inert and critically affect E-AB signaling.

One caveat to employing methyl-terminated monolayers for the fabrication of E-AB sensors is that they are prone to the nonspecific adsorption of proteins in biological fluids.[39] Because our goal is to achieve multiday E-AB sensing in vivo, we wanted to determine the effect of having methyl-terminated SAMs on E-AB signaling in serum and blood. To test this effect, we prepared aminoglycoside-binding E-AB sensors functionalized with either MCH or HxSH, immersed them in undiluted serum or blood and built calibration curves by challenging them with increasing concentrations of tobramycin. The resulting curves revealed that MCH-modified E-AB sensors still respond to target in this medium, albeit with a one-order-of-magnitude worsening of the apparent dissociation constant, going from a K_D = 154 ± 2 μM in phosphate-buffered saline to a K_D = 1.65 ± 0.05 mM in serum (Figure 6A). In contrast, HxSH-modified E-AB sensors were only modestly responsive, producing E-AB currents that decreased with increasing target concentrations irrespective of square-wave interrogation frequency (Figure 6B). In this latter case, the current progressively dropped with increasing tobramycin concentrations to a plateau at 100 μM. However, because we observed a lack of square-wave frequency-dependent behavior in this calibration, we attribute the drop in E-AB signal to the nonspecific adsorption of proteins to the sensor surface throughout the calibration, which seems to severely hinder electron transfer from the aptamer's reporter to the electrode surface.

Combining MCH and HxSH monolayers achieves full recovery of E-AB signaling in serum relative to HxSH-only monolayers. To reveal this effect, we fabricated aminoglycoside-binding E-AB sensors by incubating them in mixed solutions with different molar fractions of MCH and HxSH. At the optimal molar ratio of 1:10 MCH:HxSH, challenging the sensors with target produced full recovery of E-AB signaling relative to HxSH-only monolayers (Figure 6C). We also observed a 50% improvement in dissociation constant over MCH-only monolayers (K_D = 745 ± 35 μM). Upon repeating these experiments in whole blood, we observed a similar E-AB signal recovery, but here without the improvement in K_D (K_D ~ 1 mM, Figure S6). These results suggest that working with mixed monolayers could be an effective approach to extending the operational life of E-AB sensors while retaining antifouling properties and achieving optimal signaling.

The increased stability of methyl- over hydroxyl-terminated monolayers remains true in serum and whole blood at physiological temperatures. To demonstrate this stability, we fabricated E-AB sensors employing either MCH, HxSH, or a 1:10 MCH:HxSH mixed SAM. We then immersed these sensors in serum or whole blood in a thermally controlled cell

https://dx.doi.org/10.1021/acsami.9b22385
ACS Appl. Mater. Interfaces 2020, 12, 11214−11223

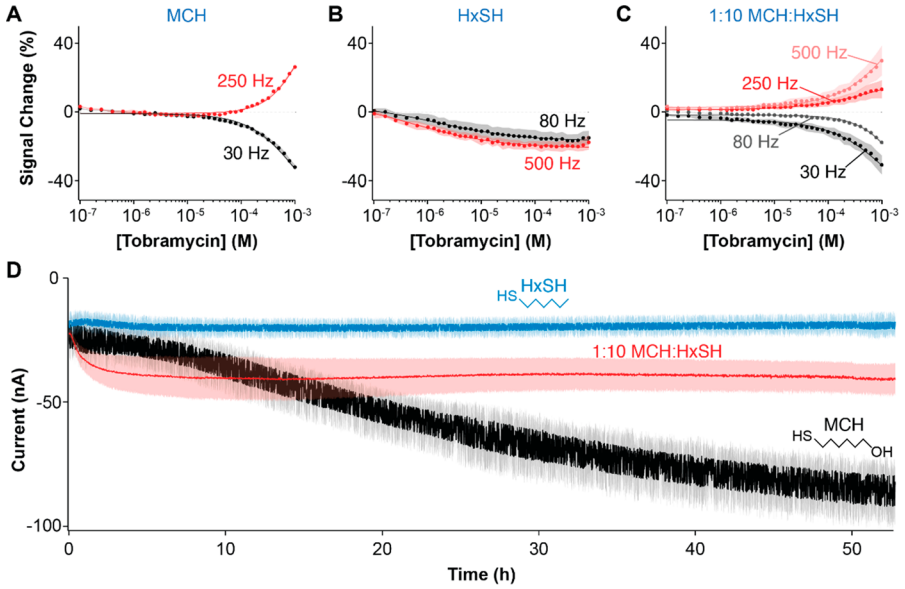

Figure 6. Monolayer end group chemistries can be tuned to enhance E-AB signaling in undiluted serum. We present calibration curves for aminoglycoside-binding E-AB sensors functionalized with (A) MCH, (B) HxSH and (C) 1:10 MCH:HxSH SAMs. Although E-AB signaling is lost on HxSH-only monolayers, we are able to fully recover E-AB signaling by preparing a mixed monolayer containing a small fraction of MCH in HxSH. Moreover, the mixed monolayer shows a 50% improvement in K_D relative to MCH-only monolayers and presents square-wave frequency dependence intermediate to MCH and HxSH-only monolayers, even at only 10% MCH. (D) While testing the operational stability of the mixed monolayer against that of MCH or HxSH-only monolayers, we observed a change in charging current, suggesting a rapid reorganization of the mixed SAM, followed by a period of stability that lasted over 2 days. Shaded areas in all panels represent the standard deviation calculated from eight electrodes. Solid lines represent nonlinear fits of the data to the Hill isotherm.

at 37 °C and serially interrogated them by cyclic voltammetry every 40 s for 50 h. By monitoring the current at voltage $P = -0.4$ V in the resulting cyclic voltammograms (for reference regarding P, see Figure 2A), we determined the rate of monolayer desorption for each of the three SAMs. Doing so, we established that HxSH SAMs remain stable and virtually unchanged for the entire measurement period (Figure 6D, blue trace). MCH SAMs, in contrast, undergo progressive desorption (Figure 6D, black trace) almost as soon as the sensors are deployed in serum, with complete loss of electrode coverage within 2 days of continuous voltammetric interrogation. Unsurprisingly, when using a mixed 1:10 MCH:HxSH monolayer, we observed an intermediate behavior containing features from both SAMs (Figure 6D, red trace). Specifically, during the first 3 h we observe a rapid transition from low to higher charging current, indicating a significant reorganization of the SAM. This rapid reorganization is presumably due to dynamic movements of the surface-bound thiols to disperse or agglomerate MCH groups, a phenomenon observed in previous works reporting on mixed monolayer.[40] After this transition ends, however, we see no changes in the measured current; we observe similar trends upon repeating these experiments with E-AB sensors immersed in whole blood (Figure S7), suggesting the use of mixed monolayers as an effective approach to extend the operational life of E-AB sensors.

CONCLUSION

We have compared the effect that two monolayer end groups, methyl and hydroxyl, have on the operational stability and signaling of E-AB sensors. Our results indicate that methyl-terminated SAMs achieve longer lasting chemical stability in biological fluids, even under continuous electrochemical interrogation, allowing E-AB sensing for periods of days without significant loss of monolayer electrode coverage. We have also observed an enhancement in the total current measured on methyl relative to hydroxyl-terminated SAMs, which is retained at all square-wave interrogation frequencies. We speculate that this current enhancement originates from the ability of the aptamer receptor to closely approach the electrode in the absence of electrostatic repulsion between, for example, the oxygen in hydroxyl-terminated monolayers and the phosphate backbone of the aptamer. Additionally, the change in monolayer end groups causes a dramatic change in E-AB signaling, in some cases shifting the apparent K_D (such as in the case of the aminoglycoside-binding aptamer), while for others (for example, doxorubicin and vancomycin aptamers), inverting the frequency dependence of E-AB signaling. We believe these effects are due to monolayer-induced changes in the folded state of the aptamer. The folded states should be affected, we speculate, by hydrogen bonding with hydroxyl groups in MCH or by changes in the potential of zero charge between the different monolayer chemistries. Moreover, the more hydrophobic HxSH monolayer could possibly cause a change in the hydration layer or reorganizational energy of the redox reporter, also altering the electron transfer kinetics of E-AB sensors. These changes in signaling notwithstanding, here we demonstrate that preparing a mixed monolayer at a molar ratio of 1:10 MCH:HxSH achieves full E-AB signaling relative to MCH.

The results presented in this work bring attention to the chemical problems underlying the relatively short operational life of E-AB sensors and point in the direction of new strategies to improve E-AB monolayer chemistries and, with them, the operational life of these sensors. Specifically, the surface-desorption resistance of thiol−gold bonds in methyl-terminated SAMs offers a new arena to study the time-dependent degradation of other components of the E-AB

https://dx.doi.org/10.1021/acsami.9b22385
ACS Appl. Mater. Interfaces 2020, 12, 11214−11223

platform. By eliminating the monolayer desorption seen with MCH SAMs (which causes the time-dependent increase in charging current seen in Figure 4C insets), HxSH reveals a clear progressive decay in the peak current of square-wave voltammograms with time. Of note is the fact that this decay is happening in buffered saline, and that it presumably is worse in biological fluids. This current decay can exclusively be attributed to the progressive loss of redox reporters from the surface of the E-AB sensor, as result of either degradation of the aptamer receptor or linker chemistries, or of the redox reporter itself (here methylene blue). Further explorations of the stability of such sensor elements are critical to achieving multiday E-AB sensing, and they are now possible to study with the use of HxSH for the passivating SAM.

METHODS

Chemicals and Materials. 6-Mercapto-1-hexanol (MCH), 1-hexanethiol (HxSH), 8-mercapto-1-octanol, 1-octanethiol, and tris(2-carboxyethyl)phosphine hydrochloride (TCEP) were purchased from Sigma-Aldrich (St. Louis, MO). Phosphate buffered saline (PBS, 11.9 mM HPO_3^{2-}; 137 mM NaCl; 2.7 mM KCl; pH = 7.4) trace-metal grade sulfuric acid (H_2SO_4), sodium hydroxide (NaOH), doxorubicin HCl, and 200 proof ethanol were purchased from Fisher Scientific (Waltham, MA). Vancomycin HCl was purchased from Alfa-Aesar (Ward Hill, MA). Tobramycin sulfate was purchased from GoldBio (St. Louis, MO). Biological fluids were purchased from BioreclamationIVT (Washington, DC). We prepared all aqueous solutions using deionized water from a Milli-Q Direct purification system, with a resistivity of 18 MΩ. Gold working electrodes (PN 002314, diameter 1.6 mm) and coiled platinum wire counter electrodes (PN 012961) were obtained from ALS Inc. (Tokyo, Japan). Silver/silver chloride reference electrodes (PN CHI111) were purchased from CH Instruments (Austin, TX). For polishing electrodes, 1200/P2500 silicon carbide grinding paper (PN 36-08-1200) was bought from Buehler (Lake Bluff, IL); cloth pads (PN: MF-1040) and alumina slurry (PN CF-1050) were purchased from BASi (West Lafayette, IN). Oligonucleotides, modified on the 5′ end with hexanethiol and on the 3′ end with methylene blue were purchased from and HPLC purified by Sigma-Aldrich (Houston, TX). The oligonucleotide modifications employed in this work had the following structures:

Hexanethiol modification at the 5' terminus:

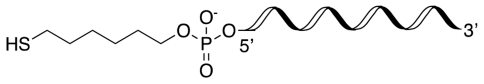

Methylene blue (MB) modification at the 3' terminus:

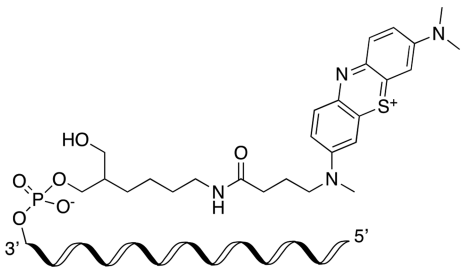

To prepare the DNA solutions, we first incubated 1 μL of 100 μM thiolated MB-modified DNA with 2 μL of 5 mM TCEP to reduce the disulfide bond. We then diluted the DNA with freshly prepared 1 mM thiol solution to a final concentration of 500 nM, as determined via molecular absorbance measurements employing an Implen Nanophotometer NP80.

Electrode Preparation. Gold electrodes were polished for ∼2 min on 1200/P2500 silicon carbide grinding paper and subsequently for ∼4 min on a cloth pad with alumina slurry. After being rinsed with water to remove polishing debris, they were then electrochemically cleaned in 0.5 M NaOH and 0.5 M H_2SO_4 following a previously reported protocol.[41] Briefly, (1) in 0.5 M NaOH, we scanned from −1 to −1.8 V vs Ag/AgCl, 300 times at a scan rate of 1 V/s; (2) in 0.5 M H_2SO_4, we scanned from +0.4 to −0.5 to +1.75 V and back to +0.4 V vs Ag/AgCl, 200 times at a scan rate of 1 V/s. Once electrodes were clean, we rinsed them with water and placed them immediately into 1 mM alkanethiol solutions with or without DNA, in either water or ethanol for 3, 15, or 24 h. We prepared sensors via coincubation, which produced identical E-AB surfaces relative to the two-step monolayer deposition typically reported in the literature; that is, a DNA incubation step followed by backfilling with a blocking monolayer.[41] Post incubation, we rinsed electrodes with water and placed them into a custom, water jacketed electrochemical cell containing 1× PBS, serum, or blood. The cell was kept at a constant temperature of either 22 or 37 °C by running temperature-controlled water through the cell jacket using a Huber Microprocessor Control MPC water recirculation bath.

Electrochemical Measurements. A CH Instruments Electrochemical Analyzer (CHI 1040C, Austin, TX) multichannel potentiostat and associated software was used for all CV and SWV measurements. We used a three-electrode cell configuration consisting of gold disk working, coiled platinum wire counter, and Ag/AgCl (saturated KCl) reference electrodes. All cyclic voltammetry measurements were recorded at a scan rate of 100 mV/s in the potential window −0.5 to +0.3 V after a 3 s quiet time, sampling current every millisecond. SWV measurements were performed from 0 to −0.5 V vs Ag/AgCl with a square-wave amplitude of 25 mV, step size of 1 mV, and various frequencies. The temperature of the electrochemical cell was held constant by a Huber Microprocessor Control MPC water recirculation bath (Huber, Cary, NC).

Data Analysis. We employed a previously reported, open-source Python script called SACMES[32] for the batch processing of our electrochemical measurements. SACMES supports the analysis of CVs and SWVs under different modalities and allows us to extract specific capacitive and faradaic currents from our electrochemical measurements, including peak areas and heights, in real time. We determined dissociation constants for each sensor architecture using the specific frequency data producing the best fit to the Hill equation. We employed the nonlinear regression function Igor Pro v8 graphing software to determine K_D values.

ASSOCIATED CONTENT

Supporting Information

The Supporting Information is available free of charge at https://pubs.acs.org/doi/10.1021/acsami.9b22385.

Literature search information used to build Panel B of Figure 1; figure showing incubation times, solvent effect of monolayer packing and stability, Aptamer probe surface density, quasi-reversible maximum maps, calibration in whole blood with different monolayers, and long-term stability of monolayers in blood (PDF)

AUTHOR INFORMATION

Corresponding Author

Netzahualcóyotl Arroyo-Currás − *Department of Pharmacology and Molecular Sciences, Johns Hopkins University School of Medicine, Baltimore, Maryland 21202, United States; Department of Chemical and Biomolecular Engineering, Whiting School of Engineering, Johns Hopkins University, Baltimore, Maryland 21218, United States;* orcid.org/0000-0002-2740-6276; Phone: 443-287-4798; Email: netzarroyo@jhmi.edu

Authors

Alexander Shaver − *Department of Pharmacology and Molecular Sciences, Johns Hopkins University School of*

https://dx.doi.org/10.1021/acsami.9b22385
ACS Appl. Mater. Interfaces 2020, 12, 11214−11223

Medicine, Baltimore, Maryland 21202, United States; orcid.org/0000-0002-5478-5291

Samuel D. Curtis − *Department of Pharmacology and Molecular Sciences, Johns Hopkins University School of Medicine, Baltimore, Maryland 21202, United States*

Complete contact information is available at: https://pubs.acs.org/10.1021/acsami.9b22385

Author Contributions

A.S. and N.A.C. developed the idea. A.S. fabricated electrodes and performed all experiments. S.D.C. wrote software in the Python programming language to enable the fast processing of datafiles generated in this work. All authors participated in the writing and editing of this manuscript.

Notes

The authors declare no competing financial interest.

■ ACKNOWLEDGMENTS

N.A.C. thanks Oak Ridge Associated Universities for granting a 2019 Ralph E. Powe Junior Faculty Enhancement Award to support this work.

■ REFERENCES

(1) Chapman, R. G.; Ostuni, E.; Takayama, S.; Holmlin, R. E.; Yan, L.; Whitesides, G. M. Surveying for Surfaces That Resist the Adsorption of Proteins [3]. *J. Am. Chem. Soc.* **2000**, *122* (34), 8303−8304.

(2) Prime, K. L.; Whitesides, G. M. Adsorption of Proteins onto Surfaces Containing End-Attached Oligo(Ethylene Oxide): A Model System Using Self-Assembled Monolayers. *J. Am. Chem. Soc.* **1993**, *115* (23), 10714−10721.

(3) Whitesides, G. M.; Prime, K. L. Self-Assembled Organic Monolayers: Model Systems for Studying Adsorption of Proteins at Surfaces. *Science (Washington, DC, U. S.)* **1991**, *252* (5009), 1164−1167.

(4) Li, H.; Dauphin-Ducharme, P.; Arroyo-Currás, N.; Tran, C. H.; Vieira, P. A.; Li, S.; Shin, C.; Somerson, J.; Kippin, T. E.; Plaxco, K. W. A Biomimetic Phosphatidylcholine-Terminated Monolayer Greatly Improves the In Vivo Performance of Electrochemical Aptamer-Based Sensors. *Angew. Chem., Int. Ed.* **2017**, *56* (26), 7492−7495.

(5) Liu, B.; Bard, A. J.; Mirkin, M. V.; Creager, S. E. Electron Transfer at Self-Assembled Monolayers Measured by Scanning Electrochemical Microscopy. *J. Am. Chem. Soc.* **2004**, *126* (5), 1485−1492.

(6) Rowe, G. K.; Creager, S. E. Chain Length and Solvent Effects on Competitive Self-Assembly of Ferrocenylhexanethiol and 1-Alkanethiols onto Gold. *Langmuir* **1994**, *10* (4), 1186−1192.

(7) Agonafer, D. D.; Chainani, E.; Oruc, M. E.; Lee, K. S.; Shannon, M. A. Study of Insulating Properties of Alkanethiol Self-Assembled Monolayers Formed Under Prolonged Incubation Using Electrochemical Impedance Spectroscopy. *J. Nanotechnol. Eng. Med.* **2012**, *3* (3), 031006.

(8) Finklea, H. O.; Avery, S.; Lynch, M.; Furtsch, T. Blocking Oriented Monolayers of Alkyl Mercaptans on Gold Electrodes. *Langmuir* **1987**, *3* (3), 409−413.

(9) Chailapakul, O.; Xu, C.; Crooks, R. M.; Sun, L. Interactions between Organized, Surface-Confined Monolayers and Vapor-Phase Probe Molecules. 7. Comparison of Self-Assembling n-Alkanethiol Monolayers Deposited on Gold from Liquid and Vapor Phases. *J. Am. Chem. Soc.* **1993**, *115* (26), 12459−12467.

(10) Muglali, M. I.; Bashir, A.; Rohwerder, M. A Study on Oxygen Reduction Inhibition at Pyridine-Terminated Self Assembled Monolayer Modified Au(111) Electrodes. *Phys. Status Solidi A* **2010**, *207* (4), 793−800.

(11) Schoukroun-Barnes, L. R.; Macazo, F. C.; Gutierrez, B.; Lottermoser, J.; Liu, J.; White, R. J. Reagentless, Structure-Switching, Electrochemical Aptamer-Based Sensors. *Annu. Rev. Anal. Chem.* **2016**, *9* (1), 163−181.

(12) Kang, D.; Ricci, F.; White, R. J.; Plaxco, K. W. Survey of Redox-Active Moieties for Application in Multiplexed Electrochemical Biosensors. *Anal. Chem.* **2016**, *88* (21), 10452−10458.

(13) Baker, B. R.; Lai, R. Y.; Wood, M. S.; Doctor, E. H.; Heeger, A. J.; Plaxco, K. W. An Electronic, Aptamer-Based Small-Molecule Sensor for the Rapid, Label-Free Detection of Cocaine in Adulterated Samples and Biological Fluids. *J. Am. Chem. Soc.* **2006**, *128* (10), 3138−3139.

(14) Schoukroun-Barnes, L. R.; Wagan, S.; White, R. J. Enhancing the Analytical Performance of Electrochemical RNA Aptamer-Based Sensors for Sensitive Detection of Aminoglycoside Antibiotics. *Anal. Chem.* **2014**, *86* (2), 1131−1137.

(15) Phares, N.; White, R. J.; Plaxco, K. W. Improving the Stability and Sensing of Electrochemical Biosensors by Employing Trithiol-Anchoring Groups in a Six-Carbon Self-Assembled Monolayer. *Anal. Chem.* **2009**, *81* (3), 1095−1100.

(16) Chidsey, C. E. D.; Loiacono, D. N. Chemical Functionality in Self-Assembled Monolayers: Structural and Electrochemical Properties. *Langmuir* **1990**, *6* (3), 682−691.

(17) Watkins, H. M.; Ricci, F.; Plaxco, K. W. Experimental Measurement of Surface Charge Effects on the Stability of a Surface-Bound Biopolymer. *Langmuir* **2018**, *34* (49), 14993−14999.

(18) Srisombat, L.; Jamison, A. C.; Lee, T. R. Stability: A Key Issue for Self-Assembled Monolayers on Gold as Thin-Film Coatings and Nanoparticle Protectants. *Colloids Surf., A* **2011**, *390* (1−3), 1−19.

(19) Lai, R. Y.; Seferos, D. S.; Heeger, A. J.; Bazan, G. C.; Plaxco, K. W. Comparison of the Signaling and Stability of Electrochemical DNA Sensors Fabricated from 6- or 11-Carbon Self-Assembled Monolayers. *Langmuir* **2006**, *22* (25), 10796−10800.

(20) Arroyo-Currás, N.; Somerson, J.; Vieira, P. A.; Ploense, K. L.; Kippin, T. E.; Plaxco, K. W. Real-Time Measurement of Small Molecules Directly in Awake, Ambulatory Animals. *Proc. Natl. Acad. Sci. U. S. A.* **2017**, *114* (4), 645−650.

(21) Schoukroun-Barnes, L. R.; Glaser, E. P.; White, R. J. Heterogeneous Electrochemical Aptamer-Based Sensor Surfaces for Controlled Sensor Response. *Langmuir* **2015**, *31* (23), 6563−6569.

(22) Li, H.; Arroyo-Currás, N.; Kang, D.; Ricci, F.; Plaxco, K. W. Dual-Reporter Drift Correction To Enhance the Performance of Electrochemical Aptamer-Based Sensors in Whole Blood. *J. Am. Chem. Soc.* **2016**, *138* (49), 15809−15812.

(23) White, R. J.; Plaxco, K. W. Exploiting Binding-Induced Changes in Probe Flexibility for the Optimization of Electrochemical Biosensors. *Anal. Chem.* **2010**, *82*, 73−76.

(24) Ferguson, B. S.; Hoggarth, D. A.; Maliniak, D.; Ploense, K.; White, R. J.; Woodward, N.; Hsieh, K.; Bonham, A. J.; Eisenstein, M.; Kippin, T. E.; Plaxco, K. W.; Soh, H. T. Real-Time, Aptamer-Based Tracking of Circulating Therapeutic Agents in Living Animals. *Sci. Transl. Med.* **2013**, *5* (213), 165.

(25) Xiao, Y.; Lubin, A. A.; Heeger, A. J.; Plaxco, K. W. Label-Free Electronic Detection of Thrombin in Blood Serum by Using an Aptamer-Based Sensor. *Angew. Chem., Int. Ed.* **2005**, *44* (34), 5456−5459.

(26) Boon, E. M.; Livingston, A. L.; Chmiel, N. H.; David, S. S.; Barton, J. K. DNA-Mediated Charge Transport for DNA Repair. *Proc. Natl. Acad. Sci. U. S. A.* **2003**, *100* (22), 12543−12547.

(27) Brust, M.; Fink, J.; Bethell, D.; Schiffrin, D. J.; Kiely, C. Synthesis and Reactions of Functionalised Gold Nanoparticles. *J. Chem. Soc., Chem. Commun.* **1995**, *5* (16), 1655−1656.

(28) Ricci, F.; Zari, N.; Caprio, F.; Recine, S.; Amine, A.; Moscone, D.; Palleschi, G.; Plaxco, K. W. Surface Chemistry Effects on the Performance of an Electrochemical DNA Sensor. *Bioelectrochemistry* **2009**, *76* (1−2), 208−213.

(29) Poirier, G. E. Characterization of Organosulfur Molecular Monolayers on Au(111) Using Scanning Tunneling Microscopy. *Chem. Rev.* **1997**, *97* (4), 1117−1128.

(30) Poirier, G. E.; Pylant, E. D.; White, J. M. Crystalline Structures of Pristine and Hydrated Mercaptohexanol Self-Assembled Monolayers on Au(111). *J. Chem. Phys.* **1996**, *105* (5), 2089−2092.
(31) Fies, W. A.; Dugger, J. W.; Dick, J. E.; Wilder, L. M.; Browning, K. L.; Doucet, M.; Browning, J. F.; Webb, L. J. Direct Measurement of Water Permeation in Submerged Alkyl Thiol Self-Assembled Monolayers on Gold Surfaces Revealed by Neutron Reflectometry. *Langmuir* **2019**, *35* (16), 5647−5662.
(32) Curtis, S. D.; Ploense, K. L.; Kurnik, M.; Ortega, G.; Parolo, C.; Kippin, T. E.; Plaxco, K. W. Open Source Software for the Real-Time Control, Processing, and Visualization of High-Volume Electrochemical Data. *Anal. Chem.* **2019**, *91*, 12321−12328.
(33) Poirier, G. E.; Pylant, E. D. The Self-Assembly Mechanism of Alkanethiols on Au (111). *Science* **1996**, *272* (5265), 1145−1148.
(34) Yeon, H.; Wang, C.; Van Lehn, R. C.; Abbott, N. L. Influence of Order within Nonpolar Monolayers on Hydrophobic Interactions. *Langmuir* **2017**, *33*, 4628−4637.
(35) Dauphin-Ducharme, P.; Zhang, Y.; Gerson, J.; Kurnik, M.; Kippin, T. E.; Stojanovic, M. N. Electrochemical Aptamer-Based Sensors for Improved Therapeutic Drug Monitoring and High-Precision, Feedback-Controlled Drug Delivery. *ACS Sensors* **2019**, *4* (10), 2832−2837.
(36) Li, H.; Dauphin-Ducharme, P.; Ortega, G.; Plaxco, K. W. Calibration-Free Electrochemical Biosensors Supporting Accurate Molecular Measurements Directly in Undiluted Whole Blood. *J. Am. Chem. Soc.* **2017**, *139*, 11207−11213.
(37) Lovrić, M.; Komorsky-Lovric, Š. Square-Wave Voltammetry of an Adsorbed Reactant. *J. Electroanal. Chem. Interfacial Electrochem.* **1988**, *248* (2), 239−253.
(38) Komorsky-Lovrić, Š.; Lovrić, M. Measurements of Redox Kinetics of Adsorbed Azobenzene by "a Quasireversible Maximum" in Square-Wave Voltammetry. *Electrochim. Acta* **1995**, *40* (11), 1781−1784.
(39) Ostuni, E.; Grzybowski, B. A.; Mrksich, M.; Roberts, C. S.; Whitesides, G. M. Adsorption of Proteins to Hydrophobic Sites on Mixed Self-Assembled Monolayers. *Langmuir* **2003**, *19* (1), 1861−1872.
(40) Schulze, E.; Stein, M. Simulation of Mixed Self-Assembled Monolayers on Gold: Effect of Terminal Alkyl Anchor Chain and Monolayer Composition. *J. Phys. Chem. B* **2018**, *122*, 7699−7710.
(41) Xiao, Y.; Lai, R. Y.; Plaxco, K. W. Preparation of Electrode-Immobilized, Redox-Modified Oligonucleotides for Electrochemical DNA and Aptamer-Based Sensing. *Nat. Protoc.* **2007**, *2* (11), 2875−2880.

https://dx.doi.org/10.1021/acsami.9b22385
ACS Appl. Mater. Interfaces 2020, 12, 11214−11223